Int. J. Heat Mass Transfer. Vol. 14, pp. 1843–1851. Pergamon Press 1971. Printed in Great Britain.

HEAT CONDUCTION CALCULATION FOR A MODEL OF THE SURFACE OF THE MOON

MEI-KAO LIU and F. A. WILLIAMS

Department of the Aerospace and Mechanical Engineering Sciences, University of California, San Diego, La Jolla, California, U.S.A.

(*Received* 18 *December* 1970 *and in revised form* 8 *March* 1971)

Abstract—Four layers, a dust layer, an anorthosite layer, a basalt layer and a dunite layer, have been used to model the surface of the Moon 4·6 billion years ago. The equations describing heat conduction with or without radioactive heating have been written and Laplace transform techniques have been applied. The thermal history of the imbedded basalt-like material has been found by numerical inversion of the Laplace transform. The objective of the present analysis is to determine whether the solidification of the basalt could be delayed about 1 billion years to produce the observed age difference between the dust and the crystalline rocks found on the surface of the Moon.

NOMENCLATURE

A's, B's, integration coefficients;
a_n, b_n, radioactive heating rates;
d, thickness of the dust layer;
g, $= \bar{T}(-\ln z)$;
h_n, dimensionless radioactive decay constants;
L, combined thickness of the anorthosite and the dunite layer;
p_n, q_n, dimensionless radioactive heating rates;
S, solar heat flux;
s, Laplace transform parameter;
T, $\bar{T}$, temperatures;
$\tilde{T}$, Laplace transform of T;
t, time;
w_i, weights;
x, space coordinate;
z, $= \exp(-\tau)$.

Greek letters

α's, dimensionless diffusivities;
β, γ, dimensionless diffusivities;
ζ, η, ξ, dimensionless space coordinates;
κ's, heat diffusivities;
λ_n, radioactive heating rates;
σ, Stefan–Boltzmann constant;
τ, dimensionless time.

1. INTRODUCTION

THE ORIGIN and possible history of the Moon and its relation to the Earth and our solar system has long attracted the attention of many astrophysicists [1]. Before the Surveyor and Apollo missions, evidence for different postulations was based solely on indirect observations. The successful space program has now introduced more definite although still limited information concerning these problems.

Muller and Sjogren [2], from lunar orbital tracking data, have observed that there exist Mascons–gravitational anomalies–below the circular maria and in a few other areas. In order to support these mass concentrations, Urey [1] postulates that the Moon must have been accumulated at low temperatures and remained cold since then. The cold core theory is also supported by the absence of a bow shock wave in the lee of the solar wind [3], and stress differences within the Moon [1]. However Turkevitch *et al.* [4], through alpha-scattering analysis of the lunar materials from Surveyors V, VI and VII, find that the chemical composi-

tions resemble that of terrestrial basalts. This indicates that differentiation by melting has occurred at least in the surface layers to some depth [1]. More dramatically, Wasserburg [5] has used Rb–Sr dating methods to show that while the age of dust on the surface of the Moon is approximately 4·6 aeons (1 aeon $= 10^9$ years), fragments of crystalline rocks dispersed through the dust are about 0·95 aeons younger. Some of these interesting observations can be explained by elaborate heat–conduction calculations.

It is tentatively assumed that about 4·6 aeons ago the surface of the Moon was heated by an intense solar wind [1, 6], adiabatically compressed gases [1] or increased solar radiation during the earliest stages of solar system history [1] to raise the surface temperature above the melting point of the basalt-like materials. These basaltic materials were between an anorthosific layer and interior dunite. On the top of these was a dust layer created by collisions [15]. Our analysis is intended to show whether the low heat conductivity of the dust layer and the radioactive heating which was abundant in the basaltic materials and anorthostic layer, could have delayed the solidification of the basalt up to about 1 aeon, thereby providing the observed age difference between the rock and the dust.

Heat conduction equations have been written for each of the three layers. The basalt-like material has been treated as a discontinuity except for the radioactive heat generated. The surface boundary condition has been simplified to a constant equilibrium temperature between radiation cooling and solar heating. Laplace transform techniques have been applied to these equations. Due to the complexity, the inversion of the transform has been obtained by a numerical technique devised by Bellman [13, 14].

2. PHYSICAL MODEL

As shown in Fig. 1, we have assumed the surface of the Moon under consideration is composed of four layers: a dust layer, an anorthosite layer, a basalt layer and a dunite layer. The thin basaltic material is embedded between the second and the third layer. From the overall composition of the Moon, Wood [7] estimated that the thickness of the second layer is about one ninth that of the third layer. Similarly one could also infer the thickness of basaltic material is 1·42 per cent of the combined thickness of the second and third layers. The combined thickness will be denoted as L henceforth and the thickness of the dust layer as d.

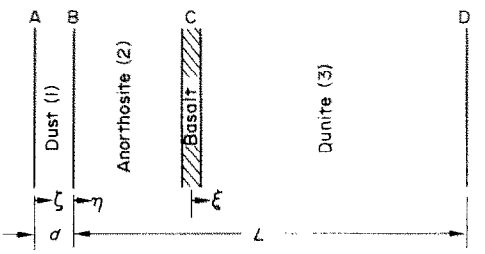

FIG. 1. A model for the surface of the moon.

The initial temperature in this surface region has been assumed to be uniformly at $T = 1300°C$, this temperature is chosen because it is the estimated solidification temperature of the anorthosite. In order to maintain a "cold core theory", the interior temperature of the Moon, T_i, can not exceed, say, 900°C. The boundary condition on the surface of the moon may have been very complicated. For instance the lunar diurnal variation must have been present. However, the lunar diurnal time scale is negligible compared to our time scale of billions of years. We have therefore used a constant equilibrium temperature,

$$T_e = \left(\frac{S}{\sigma}\right)^{\frac{1}{4}} - 273, \tag{1}$$

obtained from a balance between the solar heating and the black body radiation.

The decay constants, λ_n, of radioactive elements present on the Moon, and estimated initial heating rates of the anorthosite and basalt, denoted by a_n and b_n respectively, are tabulated in Table 1 [1].

For simplicity the physical properties will be assumed constant in the present analysis. Since we are interested only in temperatures not very different from 1300°C, this assumption should not introduce serious error. The low heat conductivity of the Moon's surface has been known for decades from the cooling curves of eclipses [1]. This has been confirmed by a measured heat diffusivity of dust samples, κ_1, of about 10^{-5} cm^2/s. On the other hand, the measured diffusivity of rock sample is 0·002 cm^2/s [8]. However it can be shown [9] that at temperatures above 1000°C, depending on the opacity of the material. the photon transport can be a competitive heat-conduction process. Therefore the measured values, which we have used, must be interpreted as lower bounds.

Table 1. *Radioactive heating constants*

Elements	λ_n (aeon^{-1})	a_n (10^{-15} °K/s)	b_n (10^{-15} °K/s)
K	0·5415	0 (A)	88·87 (A)
		0 (B)	21·82 (B)
		0 (C)	54·25 (C)
Th	0·0492	0 (A)	93·21 (A)
		8·991 (B)	18·67 (B)
		1·493 (C)	70·43 (C)
U^{235}	0·976	0 (A)	264·13 (A)
		29·39 (B)	64·17 (B)
		8·71 (C)	206·77 (C)
U^{238}	0·1537	0 (A)	135·03 (A)
		15·03 (B)	32·81 (B)
		4·45 (C)	105·71 (C)

A, B, C represent the three different rock samples.

3. MATHEMATICAL FORMULATION

The governing heat conduction equations, with a radioactive heat source in the second zone only, can be written as

$$\frac{\partial T_1}{\partial t} = \kappa_1 \frac{\partial^2 T_1}{\partial x^2} \qquad 0 \leqslant x \leqslant \mathrm{d} \tag{2}$$

$$\frac{\partial T_2}{\partial t} = \kappa_2 \frac{\partial^2 T_2}{\partial x^2} + \sum_{n=1}^{4} a_n \mathrm{e}^{-\lambda_n t} \quad 0 \leqslant x \leqslant \frac{L}{10} \tag{3}$$

$$\frac{\partial T_3}{\partial t} = \kappa_3 \frac{\partial^2 T_3}{\partial x^2} \qquad 0 \leqslant x \leqslant \frac{9L}{10}. \tag{4}$$

Subscripts 1, 2, 3, have been used to identify the dust layer, the anorthosite layer and the dunite layer respectively. The basalt layer has been treated as a discontinuity.

The initial condition is

$$T_1 = T_2 = T_3 = T_0 \quad \text{at } t = 0 \tag{5}$$

and appropriate boundary conditions are

$$T_1 = T_e \qquad @ \ A \tag{6}$$

$$T_1 = T_2 \tag{7}$$

$$\kappa_1 \frac{\partial T_1}{\partial x} = \kappa_2 \frac{\partial T_2}{\partial x} \qquad @ \ B \tag{8}$$

$$T_2 = T_3 \tag{9}$$

$$\kappa_2 \frac{\partial T_2}{\partial x} = \kappa_3 \frac{\partial T_3}{\partial x} + 0{\cdot}0142\, L \sum_{n=1}^{4} b_n e^{-\lambda_n t} \qquad @ \ C \tag{10}$$

$$T_3 = T_i \qquad @ \ D. \tag{11}$$

Conditions (9) and (11) state that temperatures are continuous and condition (8) maintains continuity of heat flux. Condition (10) specifies that the difference in heat fluxes equals radioactive heat produce in the basalt-like layer.

To facilitate Laplace transform, in the next

section we have introduced new dependent variables

$$\bar{T}_1 = T_1 - T_0$$
$$\bar{T}_2 = T_2 - T_0 \tag{12}$$
$$\bar{T}_3 = T_3 - T_0$$

and the following dimensionless variables

$$\tau = \frac{\kappa_3}{L^2}t, \quad \zeta = \frac{x}{d}, \quad \eta = \frac{10x}{L},$$
$$\xi = \frac{10x}{9L}, \quad \alpha_1 = \frac{\kappa_1 L^2}{\kappa_3 d^2}, \quad \alpha_2 = \frac{100\kappa_2}{\kappa_3},$$
$$\alpha_3 = \frac{100}{81}, \quad \beta = \frac{\kappa_1 L}{10\kappa_2 d}, \quad \gamma = \frac{9\kappa_2}{\kappa_3} \tag{13}$$
$$h_n = \frac{L^2}{\kappa_3}\lambda_n, \quad p_n = \frac{L^2}{\kappa_3}a_n, \quad q_n = 0{\cdot}01278\frac{L^2}{\kappa_3}b_n.$$

Then equations (2)–(4) yield

$$\frac{\partial \bar{T}_1}{\partial \tau} = \alpha_1 \frac{\partial^2 \bar{T}_1}{\partial \zeta^2} \qquad 0 \leqslant \zeta \leqslant 1 \tag{14}$$

$$\frac{\partial \bar{T}_2}{\partial \tau} = \alpha_2 \frac{\partial^2 \bar{T}_2}{\partial \eta^2} + \sum_{n=1}^{4} p_n e^{-h_n \tau} \qquad 0 \leqslant \eta \leqslant 1 \tag{15}$$

$$\frac{\partial \bar{T}_3}{\partial \tau} = \alpha_3 \frac{\partial^2 \bar{T}_3}{\partial \xi^2} \qquad 0 \leqslant \xi \leqslant 1 \tag{16}$$

and initial and boundary conditions (6)–(11) become

$$\bar{T}_1(\zeta, 0) = \bar{T}_2(\eta, 0) = \bar{T}_3(\xi, 0) = 0 \tag{17}$$
$$\bar{T}_1(0, \tau) = \bar{T}_e \tag{18}$$
$$\bar{T}_1(1, \tau) = \bar{T}_2(0, \tau) \tag{19}$$
$$\beta \frac{\partial \bar{T}_1}{\partial \zeta}(1, \tau) = \frac{\partial \bar{T}_2}{\partial \eta}(0, \tau) \tag{20}$$
$$\bar{T}_2(1, \tau) = \bar{T}_3(0, \tau) \tag{21}$$
$$\gamma \frac{\partial \bar{T}_2}{\partial \eta}(1, \tau) = \frac{\partial \bar{T}_3}{\partial \xi}(0, \tau) + \sum_{n=1}^{4} q_n e^{-h_n \tau} \tag{22}$$
$$\bar{T}_3(1, \tau) = \bar{T}_i. \tag{23}$$

Laplace transform and numerical inversions will be applied to the above system of equations in the next section to find the temperature at interface C as a function of time.

4. LAPLACE TRANSFORMS AND NUMERICAL INVERSIONS

The Laplace transform, defined by

$$\tilde{T}(s) = \mathscr{L}[\bar{T}(\tau)] = \int_0^\infty e^{-s\tau} \bar{T}(\tau)\, d\tau \tag{24}$$

will reduce equations (14)–(16) into a system of ordinary differential equations

$$s\tilde{T}_1 = \alpha_1 \frac{d^2 \tilde{T}_1}{d\zeta^2} \qquad 0 \leqslant \zeta \leqslant 1 \tag{25}$$

$$s\tilde{T}_2 = \alpha_2 \frac{d^2 \tilde{T}_2}{d\eta^2} + \sum_{n=1}^{4} \frac{p_n}{s + h_n} \qquad 0 \leqslant \eta \leqslant 1 \tag{26}$$

$$s\tilde{T}_3 = \alpha_3 \frac{d^2 \tilde{T}_3}{d\xi^2} \qquad 0 \leqslant \xi \leqslant 1. \tag{27}$$

The transforms of the accompanying boundary conditions (18)–(23) become

$$\tilde{T}_1(0, s) = \frac{\bar{T}_e}{s} \tag{28}$$
$$\tilde{T}_1(1, s) = \tilde{T}_2(0, s) \tag{29}$$
$$\beta \frac{d\tilde{T}_1}{d\zeta}(1, s) = \frac{d\tilde{T}_2}{d\eta}(0, s) \tag{30}$$
$$\tilde{T}_2(1, s) = \tilde{T}_3(0, s) \tag{31}$$
$$\gamma \frac{d\tilde{T}_2}{d\eta}(1, s) = \frac{d\tilde{T}_3}{d\xi}(0, s) + \sum_{n=1}^{4} \frac{q_n}{s + h_n} \tag{32}$$
$$\tilde{T}_3(1, s) = \frac{\bar{T}_i}{s}. \tag{33}$$

The solutions to equations (25)–(27) can be easily found as

$$\tilde{T}_1 = A_1 \exp\left[\sqrt{\left(\frac{s}{\alpha_1}\right)}\zeta\right] + B_1 \exp\left[-\sqrt{\left(\frac{s}{\alpha_1}\right)}\zeta\right] \tag{34}$$

$$\tilde{T}_2 = A_2 \exp\left[\sqrt{\left(\frac{s}{\alpha_2}\right)}\eta\right] + B_2 \exp\left[-\sqrt{\left(\frac{s}{\alpha_2}\right)}\eta\right] + \sum_{n=1}^{4} \frac{p_n}{s(s + h_n)} \tag{35}$$

$$\begin{bmatrix} 1 & 1 & 0 & 0 & 0 & 0 \\ e^{\sqrt{\left(\frac{s}{\alpha_1}\right)}} & e^{-\sqrt{\left(\frac{s}{\alpha_1}\right)}} & -1 & -1 & 0 & 0 \\ \beta\sqrt{\left(\frac{s}{\alpha_1}\right)}\, e^{\sqrt{\left(\frac{s}{\alpha_1}\right)}} & -\beta\sqrt{\left(\frac{s}{\alpha_1}\right)}\, e^{-\sqrt{\left(\frac{s}{\alpha_1}\right)}} & -\sqrt{\left(\frac{s}{\alpha_2}\right)} & \sqrt{\left(\frac{s}{\alpha_2}\right)} & 0 & 0 \\ 0 & 0 & -e^{\sqrt{\left(\frac{s}{\alpha_2}\right)}} & -e^{-\sqrt{\left(\frac{s}{\alpha_2}\right)}} & 1 & 1 \\ 0 & 0 & \gamma\sqrt{\left(\frac{s}{\alpha_2}\right)}\, e^{\sqrt{\left(\frac{s}{\alpha_2}\right)}} & -\gamma\sqrt{\left(\frac{s}{\alpha_2}\right)}\, e^{-\sqrt{\left(\frac{s}{\alpha_2}\right)}} & -\sqrt{\left(\frac{s}{\alpha_3}\right)} & \sqrt{\left(\frac{s}{\alpha_3}\right)} \\ 0 & 0 & 0 & 0 & e^{\sqrt{\left(\frac{s}{\alpha_3}\right)}} & e^{-\sqrt{\left(\frac{s}{\alpha_3}\right)}} \end{bmatrix} \begin{bmatrix} A_1 \\ B_1 \\ A_2 \\ B_2 \\ A_3 \\ B_3 \end{bmatrix} = \begin{bmatrix} \frac{\bar{T}_e}{s} \\ \sum_{n=1}^{4} \frac{p_n}{s(s+h_n)} \\ 0 \\ \sum_{n=1}^{4} \frac{p_n}{s(s+h_n)} \\ \sum_{n=1}^{4} \frac{q_n}{s+h_n} \\ \frac{\bar{T}_i}{s} \end{bmatrix} \tag{37}$$

$$\bar{T}_3 = A_3 \exp\left[\sqrt{\left(\frac{s}{\alpha_3}\right)}\xi\right] + B_3 \exp\left[-\sqrt{\left(\frac{s}{\alpha_3}\right)}\xi\right]. \tag{36}$$

The six unknown coefficients A's and B's can be determined by imposition of boundary conditions (28)–(33). In matrix form, the system can be expressed as shown in (37).

We are interested in the thermal history of the basalt-like material. The temperature at the interface C is

$$\begin{aligned} T_C &= T_0 + \bar{T}_2(1, \tau) \\ &= T_0 + \mathscr{L}^{-1}\left\{A_2 \exp\left[\sqrt{\left(\frac{s}{\alpha_2}\right)}\right]\right. \\ &\quad \left. + B_2 \exp\left[-\sqrt{\left(\frac{s}{\alpha_2}\right)}\right] + \sum_{n=1}^{4} \frac{p_n}{s(s + h_n)}\right\} \end{aligned} \tag{38}$$

where A_2 and B_2, being functions of s, are given by equation (37). In view of its complexity, analytical inversion of equation (38) by the Bromwich integral is not feasible. Fortunately, for certain types of problems, numerical inversions of Laplace transforms are available [12–14].

By letting $z = e^{-\tau}$, and writing $g(z) = \bar{T}(-\ln z)$ in equation (24), Bellman [13, 14] approximates the resulting integral by a Gaussian quadrature formula of degree N,

$$\begin{aligned} \bar{T}(s) &= \int_0^\infty e^{-s\tau}\, \bar{T}(\tau)\, d\tau \\ &= \int_0^1 z^{s-1}\, g(z)\, dz \\ &= \sum_{i=1}^{N} w_i z_i^{s-1}\, g(z_i) \end{aligned} \tag{39}$$

where the z_i are the zeroes of the shifted Lengendre polynomials and the w_i are the associated weights. Let s assume N different values, say $s = 1, 2, \ldots, N$, equation (39) yields a linear system of N equations in the N unknowns, $g(z_i)$. Solving this system of equations, of course, will provide the desired solution of $\bar{T}$ at N different τ's. The inverting matrix and the zeroes of the shifted Lengendre polynomials are tabulated in [13] and [14].

5. RESULTS AND DISCUSSION

The convergence for a typical numerical inversion of equation (38) is shown in Fig. 2. By using 8-, 12- and 15-point quadratures, the differences are hardly noticeable. In Fig. 3, the temperatures for three different samples of rocks are plotted against time. The two vertical bars on each curve are the estimated upper and lower bounds of the solidification temperature for basalt-like material at a depth of 100 km

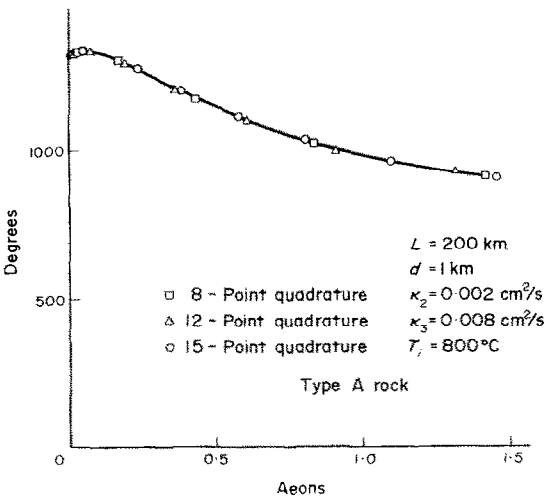

FIG. 2. Convergence of numerical inversion of Laplace transform.

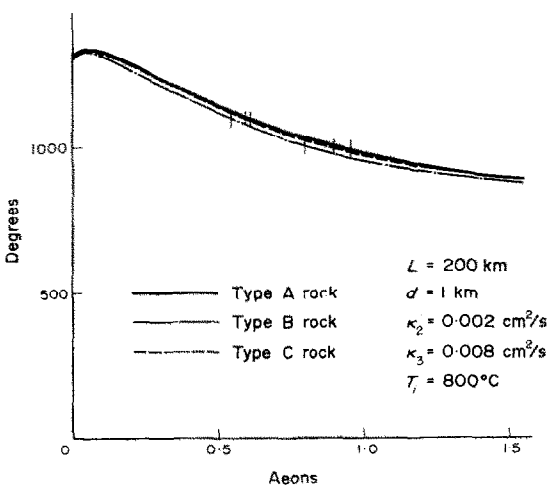

FIG. 3. Thermal histories for different rock samples.

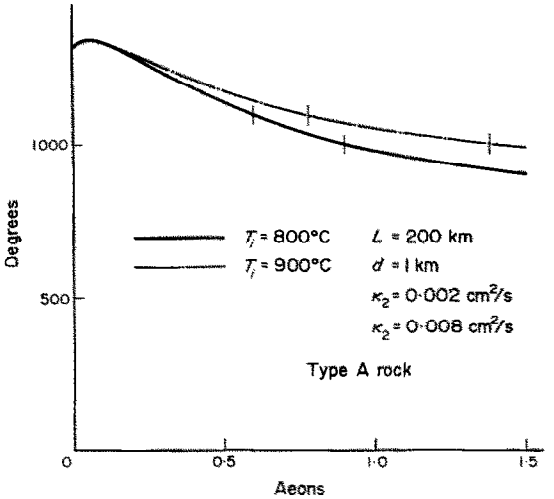

FIG. 4. Thermal history as a function of interior temperature.

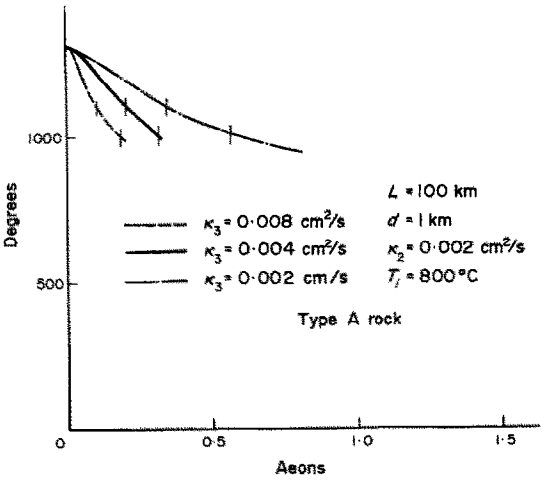

FIG. 6. Thermal history as a function of heat diffusivity, $L = 100$ km.

[1, 10]. By raising the interior temperature of the Moon from 800 to 900°C, Fig. 4 shows that solidification can be delayed from 0·78 to 1·38 aeons approximately producing the observed age difference between the dust and the rock. Calculations for $L = 200$ km and $L = 100$ km have also been made, shown in Figs. 5 and 6 respectively, with three possible values of heat diffusivity for dunite. It can be seen that, for the present model, the depth of Moon surface undergoing initial heating must exceed 100 km. However the most critical parameter, as shown in Fig. 7, is the thickness of the dust layer. The present calculation shows that this layer must be about 1 km. It has been indicated that the thickness of the dust layer of Dawes, a small crater between Mare Serenitatis and Mare Tranquillitatis, could be as thick as 1 km. Analysis of recent Apollo 12 seismic signal seems also to support the existence of a deep dust layer [11].

In conclusion, while not excluding other possible models, the present model can explain some of the surface features of the Moon.

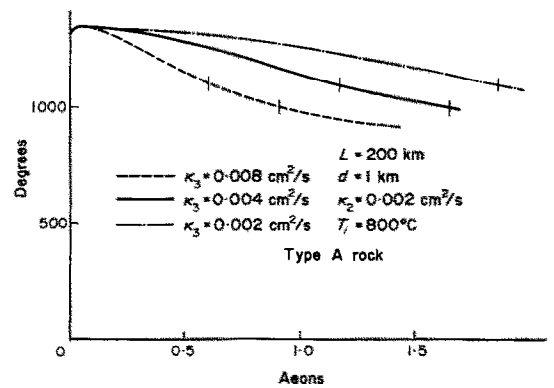

FIG. 5. Thermal history as a function of heat diffusivity, $L = 200$ km.

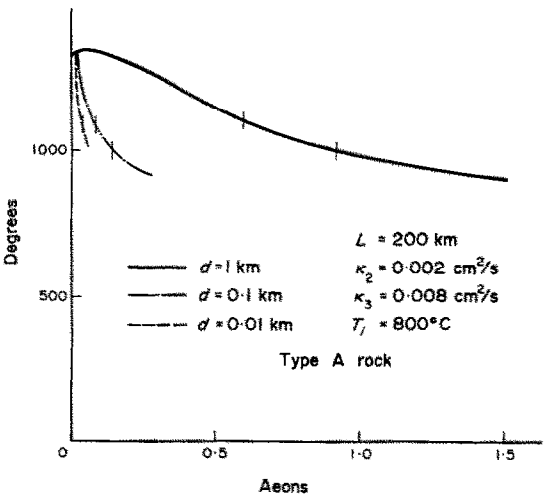

FIG. 7. Thermal history as a function of the thickness of the dust layer.

ACKNOWLEDGEMENTS

The authors are indebted to Professor Harold Urey and Professor Kurt Marti for introducing them to this interesting problem and for many fruitful discussions.

REFERENCES

1. H. C. Urey and G. J. F. MacDonald, Origin and history of the moon, Chapter 13 (Revised) of *Physics and Astronomy of the Moon*, edited by Z. Kopal, Academic Press (1970).
2. P. M. Muller and W. L. Sjogren, Mascons: lunar mass concentrations, *Science* **161**, 680 (1968).
3. N. F. Ness, K. W. Behannon, C. S. Scearce and S. C. Cantaran, Early results from the magnetic field experiment on lunar explorer 35, *J. Geophys. Res.* **72**, 5769 (1967).
4. A. L. Turkevich, E. J. Franzgrote and J. H. Paterson, Chemical analysis of the moon at the Surveyor VI landing site: Preliminary results, *Science* **160**, 1108 (1968).
5. A. L. Albee and G. J. Wasserburg, Ages, irradiation history, and chemical composition of lunar rocks from the sea of tranquillity, *Science* **167**, 463 (1970).
6. C. P. Sonett and D. S. Colburn, Establishment of a lunar unipolar generator and associated shock and wake by the solar wind, *Nature* **216**, 340 (1967).
7. J. A. Wood, The lunar soil, *Scient. Am.* **223**, 16 (1970).
8. T. Murase and A. R. McBirney, Thermal conductivity of lunar and terrestrial igneous rocks in their melting range, *Science* **170**, 165 (1970).
9. G. J. F. MacDonald, Calculations on the thermal history of the earth, *J. Geophys. Res.* **64**, 1967 (1959).
10. H. Yoder and C. Tilley, Origin of basalt magnas: An experimental study of natural and synthetic rock system, *J. Petrol.* **3**, 342 (1962).
11. T. Gold and S. Soter, Apollo 12 seismic signal: Indication of a deep layer of powder, *Science* **169**, 1071 (1970).
12. V. I. Krylov and N. S. Skoblya, *Handbook of Numerical Inversion of Laplace Transforms*. Israel Program for Scientific Translations, Jerusalem (1969).
13. R. E. Bellman, R. E. Kaiaba and J. A. Lockett, *Numerical Inversion of the Laplace Transforms*. American Elsevier, N.Y. (1966).
14. R. E. Bellman, H. H. Kagiwada, R. E. Kaiaba and M. C. Prestrud, *Invariant Imbedding and Time-Dependent Transport Processes*. American Elsevier, N.Y. (1964).
15. H. C. Urey, K. Marti, J. W. Hawkins and M. K. Liu, Model history of the lunar surface, Presented at the Apollo 12 Lunar Science Conference, Houston, Texas (January 1971).

CALCUL DE CONDUCTION THERMIQUE POUR UN MODELE DE LA SURFACE DE LA LUNE

Résumé—Quatre couches, une couche de poussière, une couche d'anorthosite, une couche de basalte, et une couche de dunite ont été utilisées comme éléments de la surface lunaire il y a 4,6 billions d'années. Les équations qui décrivent la conduction de chaleur avec ou sans chauffage radioactif ont été écrites et les techniques de la tranformation de Laplace ont été appliquées. L'histoire thermique d'un matériau de type basalte a été trouvée par inversion numérique de la transformée de Laplace. L'objectif de la présente analyse est de déterminer si la solidification du basalte pouvait être retardée d'environ un billion d'années pour réaliser la différence d'âge observée entre la poussière et les roches cristallines trouvées sur la surface de la lune.

UNTERSUCHUNGEN DER WÄRMELEITUNG AN EINEM MODELL FÜR DIE OBERFLÄCHE DES MONDES.

Zusammenfassung—Vier Schichten, eine Staub-Schicht, eine anorthosite-Schicht, eine Basalt-Schicht und eine dunite-Schicht, wurden für ein Modell verwendet, das die Mondoberfläche vor 4,6 Milliarden Jahren repräsentiert. Die beschreibenden Differentialgleichungen für die Wärmeleitung wurden mit und ohne Strahlungsterm aufgestellt und mit Hilfe der Laplace-Transformation gelöst. Durch numerische Rücktransformation der Lösung konnte die "thermische Lebensgeschichte" des eingebetteten basaltähnlichen Materials wiedergegeben werden. Das Ziel der vorliegenden Untersuchung ist die Klärung der Frage, ob sich der Erstarrungsvorgang des Basalts über 1 Milliarde Jahre hinziehen konnte, um damit das beobachtete unterschiedliche Alter zwischen Staub und den kristallinen Gesteinen auf der Oberfläche des Mondes zu erklären.

РАСЧЁТ ТЕПЛОПРОВОДНОСТИ ДЛЯ МОДЕЛИ ПОВЕРХНОСТИ ЛУНЫ

Аннотация—Используется модель лунной поверхности, имеющей возраст 4,6 биллиона лет, состоящая из четырех слоев: слоя пыли, слоя анортозита, слоя базилита и слоя

лунита. Записаны уравнения, описывающие теплопроводность при наличии и отсутствии радиоактивного нагрева. К ним применен метод преобразования Лапласа. Путем численного обращения преобразования Лапласа определена термическая история включений базальтообразного материала. Целью данного анализа является определение возможности задержки отвердевания базальта примерно на 1 биллион лет, чет, что могло бы вызвать наблюдаемую возрастную разницу между пылью и кристаллическими породами, обнаруженными на поверхности луны.